Hindawi
Advances in Astronomy
Volume 2021, Article ID 6658051, 12 pages
https://doi.org/10.1155/2021/6658051

Research Article

Chaotic Oscillation of Satellite due to Aerodynamic Torque

Rashmi Bhardwaj [1] **and Mohammad Sajid** [2]

[1]*University School of Basic and Applied Sciences, Non-Linear Dynamics Research Lab, Guru Gobind Singh Indraprastha University, Dwarka, New Delhi, India*
[2]*Department of Mechanical Engineering, College of Engineering, Qassim University, Buraidah-51452, Al Qassim, Saudi Arabia*

Correspondence should be addressed to Rashmi Bhardwaj; rashmib22@gmail.com

Received 7 December 2020; Revised 11 January 2021; Accepted 28 January 2021; Published 10 February 2021

Academic Editor: Elbaz Abouelmagd

This study presents the chaotic oscillation of the satellite around the Earth due to aerodynamic torque. The orbital plane of the satellite concurs is same as the tropical plane of Earth. The half-width of riotous separatrix is assessed utilizing Chirikov's measure. Variety of boundary techniques shows that streamlined force boundary (ε), unpredictability of circle (e), and mass-proportion (ω_0) convert normal wavering to the disorganized one. We studied the behavior of trajectories due to change in parameters with Lyapunov exponents and time series plots. The theory is applied to Resourcesat-1, an artificial satellite of the Earth.

1. Introduction

Artificial satellites are widely used in telecommunication, mass media and weather forecast, agriculture, and navigation. Satellites are widely used in agriculture and forestry for crop inventory, yield prediction, and soil/crop condition monitoring. Resourcesat-1 (also known as IRS-P6) is an advanced remote sensing satellite built by the Indian Space Research Organization (ISRO). The tenth satellite of ISRO in IRS series, Resourcesat-1, is intended to not only continue the remote sensing data services provided by IRS-1C and IRS-1D, both of which have far outlived their designed mission lives, but also vastly enhance the data quality. The major objectives of Resourcesat-1 are to provide continued remote sensing data services on operational basis for integrated land and water resources management with enhanced multispectral/spatial coverage and stereo imaging and also to develop new areas of applications to take full advantages of increased spatial and spectral resolutions. For a country like India, with populations separated by rough terrain and different languages, communications satellites provide remote populations access to education and to medical expertise that would otherwise not reach them [1].

Satellite exhibits chaotic motion under the influence of different torques and, for the low-thrust tug-debris tethered system in a Keplerian orbit, experiences chaotic attitude motion. Aslanov et al. [2] introduced steady and insecure fixed answers for the in-plane movement of the framework in a roundabout circle, which rely upon the estimation of the pull's pushed. Bhardwaj and Kaur [3] studied the satellite motion under the effect of aerodynamic torque and explained in detail about the nonresonance oscillation. Also, they discussed that under the influence of magnetic torque for different mass parameters, tumbling of satellite experiences shows the chaotic signal [4]. Bhardwaj and Sethi [5] discussed that air drag exhibits resonance criteria for nonlinear motion. Rotational nonlinear oscillation of the satellite under the influence of combined aerodynamic and magnetic torque was discussed by Bhardwaj et al. [6], and they concluded that with the change in mass parameter, the dynamics of the satellite altered. Bhardwaj and Tuli [7] discussed the nonlinear planar oscillation of a satellite under the influence of third-body torque, and it is concluded that Hyperion tumbled more chaotically with the change in the third body torque parameter. Planar oscillation of a satellite in an elliptic orbit for magnetic torque was studied by

Bhardwaj and Kaur [8], and they observed that as eccentricity changed, the oscillation of satellite exhibits chaotic motion which increases with the increase in eccentricity. Bhardwaj and Bhatnagar [9–12] studied the nonlinear planar rotational oscillation of the satellite in circular orbit for magnetic torque and for third-body torque in elliptic orbit, and it is concluded that the mass parameter and torque parameter play an important role in changing the motion from regular to the chaotic one.

Chegini et al. [13, 14] explored mathematically turmoil in demeanor elements of an adaptable satellite made out of an inflexible body and two indistinguishable unbending boards connected to the fundamental body with springs using analytical and numerical methods. Clemson and Stefanovska [15] discussed the analysis of nonautonomous dynamics for extracting properties of interactions and the direction of couplings for chaotic, stochastic, and nonautonomous behaviour. For the chaotic class, the Lorenz system; for the stochastic class, the noise forced Duffing system; and for the nonautonomous class, the Poincare oscillator with quasiperiodic forcing discussed and gave a good review to distinguish nonautonomous dynamics from chaos or stochasticity. Doroshin [16] got altered numerical models and dynamical frameworks to give an idea of heteroclinic chaos and its local suppression in attitude dynamics for dual spin spacecraft and gyrostat satellites. Gutnik and Sarychev [17] mathematically simulated the motion of the satellite under aerodynamic torque for the control system influenced by the active dumping torques. Inarrea and Lanchares [18] examined the pitch movement elements of an awry rocket in round circle affected by a gravity inclination force and accepted that shuttle is irritated by a little streamlined drag force corresponding to the precise speed of the body about its mass community. Koupriano and Shevchenko [19] considered the issue of recognizability of clamorous systems in turn of planetary satellites utilizing Jacobian assessment approach. Kuptsov and Kuznets [20] discussed the Lyapunov analysis of strange pseudohyperbolic attractors and briefly analyzed about the angles between tangent subspaces, local volume expansion, and contraction.

The phenomenon of chaos is generally related to the field of dynamical systems, and it can be characterized in the dynamics by sensitive dependence on the initial conditions. Chaos is a fascinating mathematical and physical phenomenon. The study of chaos shows that simple systems can exhibit a complex and unpredictable behaviour. The chaos in the dynamics can be identified and quantified by several techniques. A positive value of the Lyapunov exponent provides chaos in the dynamics which is discussed by Letellier [21]. Liu and Cui [22] analyzed the nonlinear model which should be adopted for the sailcraft in long duration missions, and the restricted position of the sliding mass could be selected elaborately to utilize the resultant torque by the gravitational and center-of-mass or center-of-pressure torques. Melnikov and Shevchenko [23] considered the issue of figuring the Lyapunov season of the disorganized movement region for resonances in satellite movement. Pritykin et al. [24] discussed the long-term evolution of attitude motion for defunct satellites in nearly polar orbits. Rosengren et al. [25] indicated that the sporadic and random characters of the Global Navigation Satellite Systems' circles mirror a comparative inconsistency in the circles of numerous divine bodies in our solar framework. Rawashdeh [26] studied the attitude analysis of small satellites using model-based simulation. Efimov et al. [27] discussed about long-term attitude dynamics of space debris for sun-synchronous orbits and studied about Cassini cycles and chaotic stabilization. Chang [28] gave an idea of stability, chaos detection, and quenching chaos for the swing equation system. Wang et al. [29] developed the six-dimensional hyperchaotic system and applied for secure communication circuit implementation. Wolf et al. [30] introduced the main calculations that permit the assessment of nonnegative Lyapunov types from an exploratory time arrangement.

Apparently, none of the creators have contemplated the bedlam affected by the streamlined force in an elliptic circle. In the current examination, we contemplated the tumultuous movement of a satellite affected by a streamlined force in an elliptic circle. In this study, the condition of movement for the framework is inferred. Utilizing variety of boundaries techniques, the unrest, libration, and endless period separatrix are examined. The mathematical recreation of tumultuous movement affected by the streamlined force is examined for Earth-Resourcesat-1 satellite.

2. Mathematical Model

Let an inflexible satellite S revolve in elliptic circle around Earth E with the end goal that orbital plane concurs with central plane of Earth. S is thought a trihub body with head snapshots of inactivity $A < B < C$ at its focal point of mass, and C is the snapshot of idleness about turn hub which is opposite to the orbital plane. Let $\overrightarrow{r}$ be the sweep vector of focal point of mass of S, ν be the true anomaly, θ be the point that the long hub of S makes with fixed line EF lying in the orbital plane, and $(\eta/2)$ be the point between the span vector and long pivot as shown in Figure 1.

Equation of motion for the system, see details as given in [3], is obtained as

$$\begin{aligned}\frac{d^2\eta}{d\nu^2} + n^2\eta = {} & -e\cos\nu\frac{d^2\eta}{d\nu^2} + 2e\sin\nu\frac{d\eta}{d\nu} \\ & + 4e\sin\nu + n^2(\eta - \sin\eta) \\ & + \varepsilon\left(A_*\nu^2\sin\nu + B_*\nu\sin\nu + C_*\sin\nu + D_*\nu + E_*\right),\end{aligned} \tag{1}$$

where $n^2 = ((3(B-A))/C) =$ mass parameter; $\varepsilon = ((\rho SC_d l^2)/(C\Omega^2)) =$ aerodynamic torque parameter; $A_* = ((a^2(1-e))/\Omega^2 l) =$ constant; $B_* = (((\omega a(2e-1))/\Omega)\cos i + ((2V_1 a(1-2e))/\Omega l)) =$ constant; $C_* = (\omega V_1(2e-1)\cos i + ((V_1^2(1-2e))/l) + ((\omega ae)/2\Omega)\sin i) =$ constant; $D_* = (((\omega a(2e-1))/\Omega)\sin i) =$ constant; $E_* = \omega V_1(2e-1)\sin i =$ constant; and

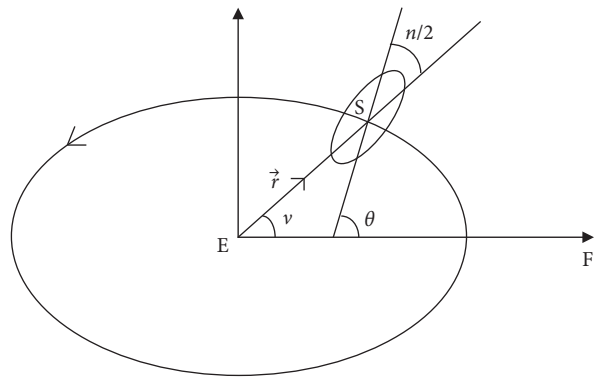

Figure 1: S revolving around Earth E.

$$\frac{d^2\theta}{dt^2} = \frac{\mu}{r^3}\left(-2e\sin\nu - e\sin\nu\frac{d\eta}{d\nu} + \frac{1}{2}(1+e\cos\nu)\frac{d^2\eta}{d\nu^2}\right). \tag{2}$$

From equations (1) and (2), we get

$$\frac{d^2\theta}{dt^2} = -\frac{\mu}{2r^3}\left(n^2\sin\delta - \varepsilon_1 \cdot \left(A_*\nu^2\sin\nu + B_*\nu\sin\nu + C_*\sin\nu + D_*\nu + E_*\right)\right). \tag{3}$$

Taking $n^2 = \omega_0^2 = ((3(B-A))/C)$; $\theta = \nu + (\delta/2) \Rightarrow \delta = 2(\theta - \nu)$, equation (3) becomes

$$\frac{d^2\theta}{dt^2} = -\frac{\mu}{2r^3}\left(\omega_0^2\sin(2(\theta-\nu)) - \varepsilon_1 \cdot \left(A_*\sin\nu^3 + B_*\sin\nu^2 + C_*\sin\nu + D_*\nu + E_*\right)\right). \tag{4}$$

In condition (4), if units are picked to the point that orbital time of S is 2π and its semisignificant pivot is 1, at that point dimensionless, time is equivalent to mean longitude or genuine inconsistency which is 2π intermittent and $\mu = 1$. As r and ν are 2π occasional as expected, utilizing Fourier-like Poisson series (Wisdom et al. [31]), equation (4) becomes

$$\frac{d^2\theta}{dt^2} + \frac{\omega_0^2}{2}\sum H\left(\frac{m}{2}, e\right)\sin(2\theta - mt) - \frac{\varepsilon}{2}\left(A_*\sin\nu^3 + B_*\sin\nu^2 + C_*\sin\nu + D_*\nu + E_*\right) = 0, \tag{5}$$

$H((m/2), e)$ corresponds to $e^{2|(m/2)-1|}$ and is given by Cayley [32] and Goldreich and Peale [33]. At the point, if e is little, $H((m/2), e) \cong -(e/2)$. The half whole number $(m/2)$ is signified by the image p. Resonances happen at whatever point one of the contentions of the sine or cosine capacities is almost fixed, for example, at whatever point $|(d\theta/dt) - p| \ll (1/2)$. In such cases, it is to rework the condition of movement as far as the gradually changing reverberation variable $\nu_p = \theta - pt \Rightarrow ((d^2\nu_p)/dt^2) = ((d^2\theta)/dt^2) \Longrightarrow 2\nu_p = 2\theta - mt$. Equation (5) can be written as

$$\frac{d^2\nu_p}{dt^2} + \frac{\omega_0^2}{2}H(p,e)\sin 2\nu_p - \frac{\varepsilon}{2}\left(A_*\sin\nu^3 + B_*\sin\nu^2 + C_*\sin\nu + D_*\nu + E_*\right) = 0. \tag{6}$$

This is pendulum perturbed by $(\varepsilon/2)(A_*\sin\nu^3 + B_*\sin\nu^2 + C_*\sin\nu + D_*\nu + E_*)$. When $\varepsilon \neq 0$, condition (6) speaks to the condition of movement of upset pendulum given by

$$\left(d^2x_p/dt^2\right) + f'\left(x_p\right) = m_p g\prime\left(x_p, t\right), \tag{7}$$

where $x_p = 2\nu_p$; $f'(x_p) = k_{1p}^2\sin x_p$; $k_{1p}^2 = \omega_0^2 H(p,e)$; $m_p = \varepsilon$; and $g'(x_p, t) = A_*\sin t^3 + B_*\sin t^2 + C_*\sin t + D_*t + E_*$. The unperturbed piece of condition (7) is $((d^2x_p)/dt^2) + f'(x_p) = 0 \Rightarrow (dx_p/dt)^2 = 2k_{1p}^2\cos x_p + c_{1p}$. The integration constant is defined as c_{1p}. If $c_{1p} + 2k_{1p}^2 \geq 0$, then motion is said to be real. Three kinds of motions are defined based on the conditions $c_{1p} > 2k_{1p}^2$, $c_{1p} < 2k_{1p}^2$, and $c_{1p} = 2k_{1p}^2$.

2.1. Category-I. We consider $c_{1p} > 2k_{1p}^2$. For $c_{1p} > 2k_{1p}^2$, the value of (dx_p/dt) never vanishes; it is either certain or negative, and the pendulum is seeming well and good or the other. For this situation, the unperturbed arrangement is

$$x_p = l_p + c_{1p}\sin l_p + o\left(c_{1p}^2\right),$$
$$l_p = n_p t + \varepsilon_1,$$
$$c_{1p} = \frac{k_{1p}^2}{n_p^2};$$
$$\frac{1}{n_p} = \frac{1}{2\pi}\int_0^{2\pi}\frac{dx_p}{\left(c_{1p} + 2k_{1p}^2\cos x_p\right)^{(1/2)}}, \tag{8}$$

Table 1: Earth-Resourcesat-1 system for fixed values of $A_* = 3.36E + 09, B_* = 1596.387, C_* = -103631, D_* = -4E + 08, E_* = 200.1022, e = 0.001, \varepsilon$, and variation in n.

Figure no.	n	ε	Graphical behaviour of Poincare map	Graphical behaviour of Lyapunov exponent
2	0.0001	0.000000000000000001	Regular curves disintegrate as ε increases	Chaotic
3		0.00000000000001		Chaotic
4	0.9	0.000000000000000001		Periodic
5		0.00000000000001		Periodic and chaotic

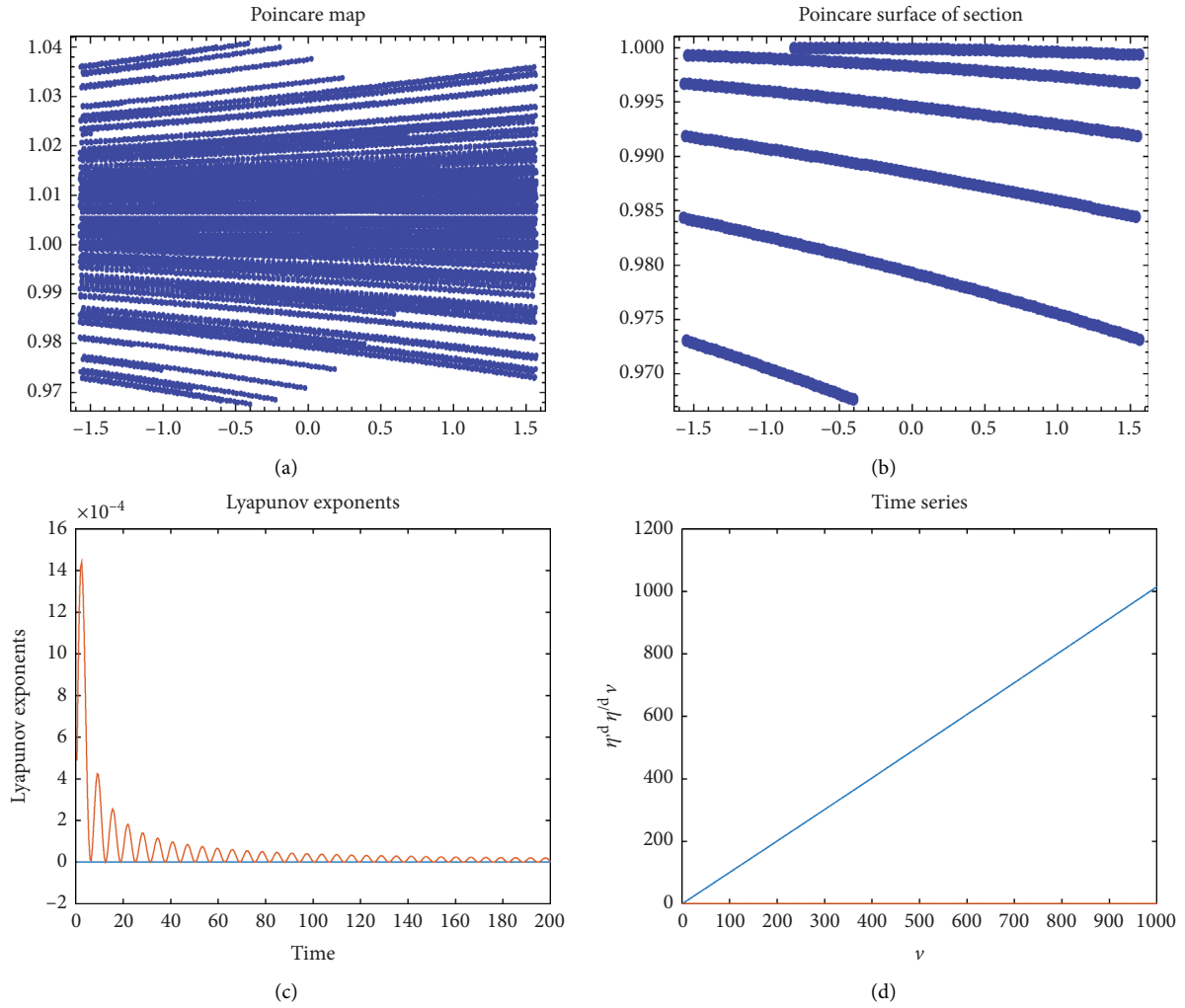

Figure 2: For $n = 0.0001, \varepsilon = 0.000000000000000001, A_* = 3.36E + 09, D_* = -4E + 08, B_* = 1596.387, C_* = -103631, E_* = 200.1022$, and $e = 0.001$. (a) Poincare map, (b) Poincare surface of section, (c) Lyapunov exponent, and (d) time series.

where c_{1p} and ε_1 are the discretionary constants, and l_p is a contention. Intermittent segment of this arrangement can be viewed as swaying about the mean condition of movement which is unrest with a period $(2\pi/n_p)$. Half plentifulness of wavering is clearly not exactly π, and it diminishes as n_p increments. Here, we may see that $(\mathrm{d}x_p/\mathrm{d}t) \neq 0$, and the movement is supposed to be of type I, for example, upheaval. Brown and Shook [34] proposed the theory of variation of parameters for the perturbed pendulum which gives

$$\frac{\mathrm{d}c_{1p}}{\mathrm{d}t} = \frac{m}{k_p}\frac{\partial x}{\partial l}g',$$

$$\frac{\mathrm{d}l_p}{\mathrm{d}t} = n - \frac{m}{k_p}\frac{\partial x}{\partial c_1}g', \tag{9}$$

$$k_p = \frac{\partial}{\partial c_{1p}}\left(n_p\frac{\partial x}{\partial l}\right)\frac{\partial x}{\partial l} - n_p\frac{\partial^2 x}{\partial l^2}\frac{\partial x}{\partial c_{1p}},$$

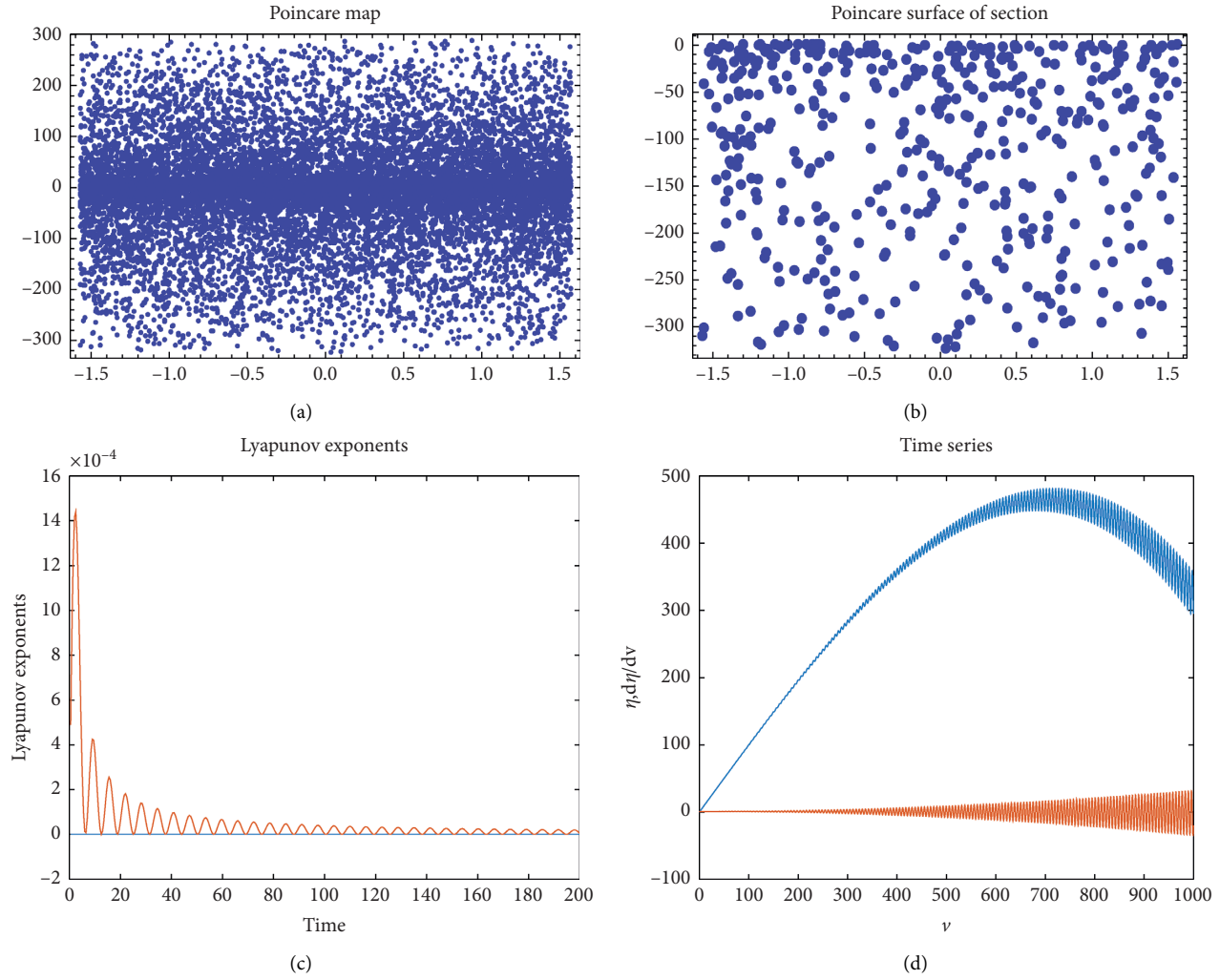

FIGURE 3: For $n = 0.0001, \varepsilon = 0.00000000000001, A_* = 3.36E+09, D_* = -4E+08, \quad B_* = 1596.387, C_* = -103631, E_* = 200.1022,$ and $e = 0.001$. (a) Poincare map, (b) Poincare surface of section, (c) Lyapunov exponent, and (d) time series.

since $c_{1p} = (k_{1p}^2/n_p^2)$. Therefore,

$$\begin{aligned}
\frac{\partial n_p}{\partial c_{1p}} &= -\frac{n_p}{2c_{1p}}, \\
\frac{\partial x_p}{\partial l_p} &= 1 + c_{1p}\cos l_p, \\
\frac{\partial^2 x_p}{\partial {l_p}^2} &= -c_{1p}\sin l_p, \\
\frac{\partial x_p}{\partial c_{1p}} &= \sin l_p, \\
\frac{\partial^2 x_p}{\partial c_{1p}\partial l_p} &= \cos l_p.
\end{aligned} \tag{10}$$

Putting the above values and writing $k_p = k_{1p}$, equation (9) can be written as

$$\begin{aligned}
k_{1p} = &-\frac{n_p}{2c_{1p}} - \frac{n_p c_{1p}\cos^2 l_p}{2} \\
&+ n_p c_{1p} \cong -\frac{n_p}{2c_{1p}}.
\end{aligned} \tag{11}$$

Hence, $(\mathrm{d}c_{1p}/\mathrm{d}t) \cong 0$; so, c_{1p} is the second order approximation constant. Second equation of (9) gives

$$\begin{aligned}
\frac{\mathrm{d}l_p}{\mathrm{d}t} = &\, n_p + \frac{2m_p c_{1p}}{n_p}\sin l_p \\
&\cdot \left(A_* \sin t^3 + B_* \sin t^2 + C_* \sin t + D_* t + E_*\right).
\end{aligned} \tag{12}$$

Rejecting second or higher order terms, we get

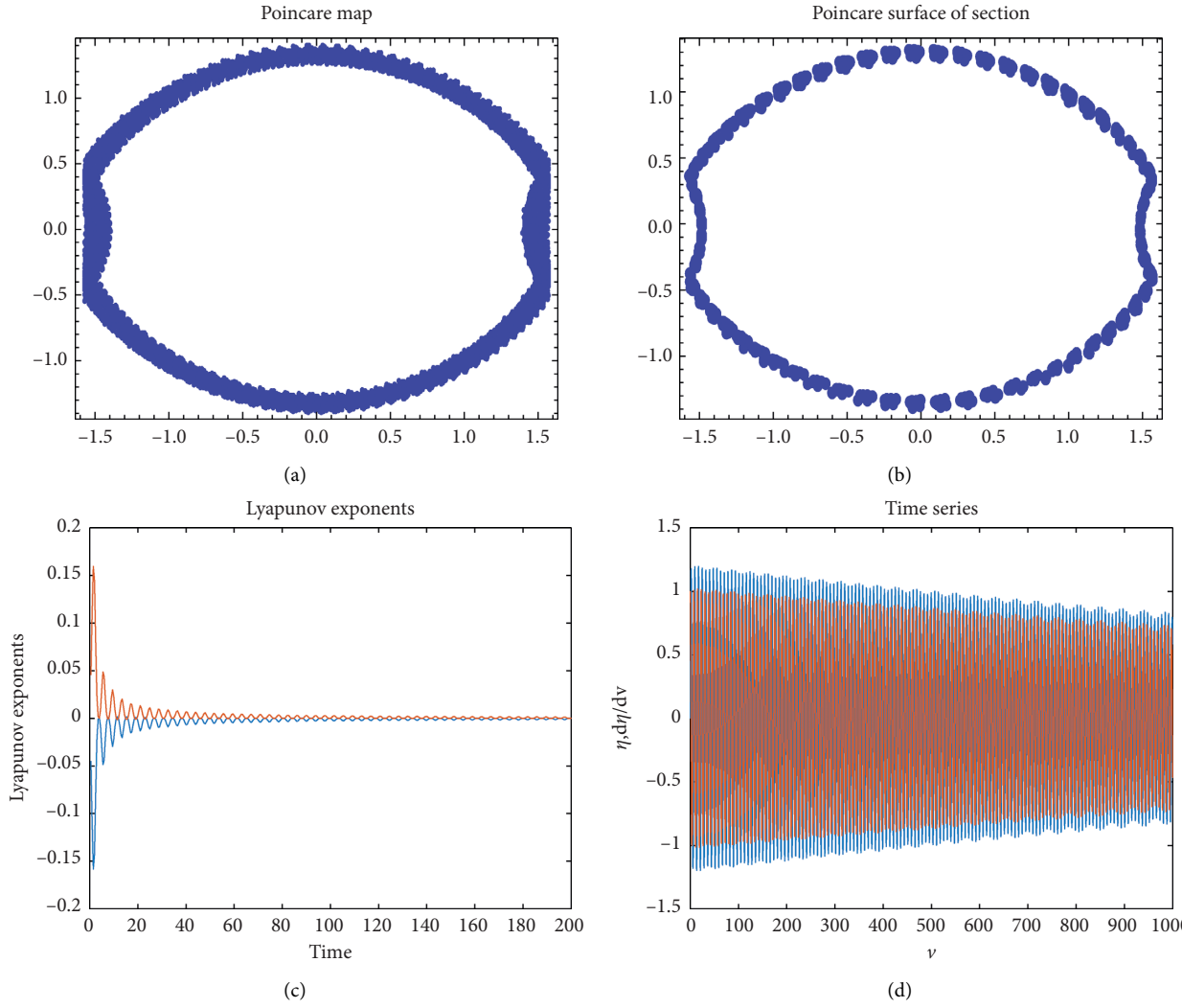

FIGURE 4: For $n = 0.9, \varepsilon = 0.000000000000000001, A_* = 3.36E + 09, D_* = -4E + 08, \quad B_* = 1596.387, C_* = -103631, E_* = 200.1022,$ and $e = 0.001$. (a) Poincare map, (b) Poincare surface of section, (c) Lyapunov exponent, and (d) time series.

$$\frac{d^2 l_p}{dt^2} = \left(\frac{2C_* m_p c_{1p}}{n_p} + \frac{2D_* m_p c_{1p}}{n_p} - \frac{6E_*^2 m_p^2 c_{1p}}{n_p^2} + \frac{4E_*^2 m_p^2 c_{1p}^2}{n_p}\right) \cdot \sin l_p + \left(1 + 2c_{1p}\right)\left(C_* m_p \sin t + D_* m_p t + E_* m_p\right),$$

$$\frac{d^2 l_p}{dt^2} + k_{2p}^2 \sin l_p = m_p\left(1 + 2c_{1p}\right)\left(C_* \sin t + D_* t + E_*\right). \tag{13}$$

Let $l_p = x_p$, $(d^2 x_p/dt^2) + k_{2p}^2 \sin x_p = m_p g\prime\prime(x_p, t)$, where $g\prime\prime(x_p, t) = (1 + 2c_{1p})(C_* \sin t + D_* t + E_*)$, and $k_{2p}^2 = -(((2C_* m_p c_{1p})/n_p) + ((2D_* m_p c_{1p})/n_p) - ((6E_*^2 m_p^2 c_{1p})/n_p) + ((4E_*^2 m_p^2 c_{1p}^2)/n_p))$. The unperturbed part of the above equation is $(d^2 x_p/dt^2) + k_{2p}^2 \sin x_p = 0 \Rightarrow (dx_p/dt)^2 = 2k_{2p}^2 \cos x_p + c_{2p}$, where c_{2p} is a constant of integration. Three types of motions are obtained for the motion of pendulum.

(1) If $(dx_p/dt) \neq 0$, then motion of type 1 exists. For type 1, the solution is $x_p = N_p t + \varepsilon_{2p} + (k_{2p}^2/N_p^2) \sin(N_p t + \varepsilon_{2p}) + \cdots$; $(1/N_p) = (1/2\pi)\int_0^{2\pi} (dx_p/(c_{2p} + 2k_{2p}^2 \cos x_p)^{(1/2)})$, where c_{2p} and ε_{2p} are the arbitrary constants. For first approximation, $N_p = N_{0p}$; so, $x_p = x_{0p} + (k_{2p}^2/N_{0p}^2)\sin(x_{0p})$, where $x_{0p} = N_{0p} t + \varepsilon_{2p}$. This is situation of unrest.

(2) If $(dx_p/dt) = 0$ at 0 or π, then motion of type 2 exists. For type 2, solution is $x_p = \lambda_p \sin(p\prime t + \lambda_0)$, where $p\prime = \sqrt{((2m_p \omega_0^2 H(p,e))/n_p^3)(C_* + D_* + ((E_*^2 m_p)/n_p)(-3 + 2((2\omega_0^2 H(p,e))/n_p^2)))}$, λ_p, λ_0 are defined as the constants of integration. This is situation of libration.

(3) Type 3 when $c_{2p} = 2k_{2p}^2 = -((4\omega_0^2 m_p H(p,e))/n_p^3)(C_* + D_* + ((E_*^2 m_p)/n_p)(2((\omega_0^2 H(p,e))/n_p^2) - 3))$. Solution is $x_p + \pi = 4\tan^{-1} \exp(k_{2p} t + \alpha_0)$. The arbitrary constant is defined as α_0. It is observed that

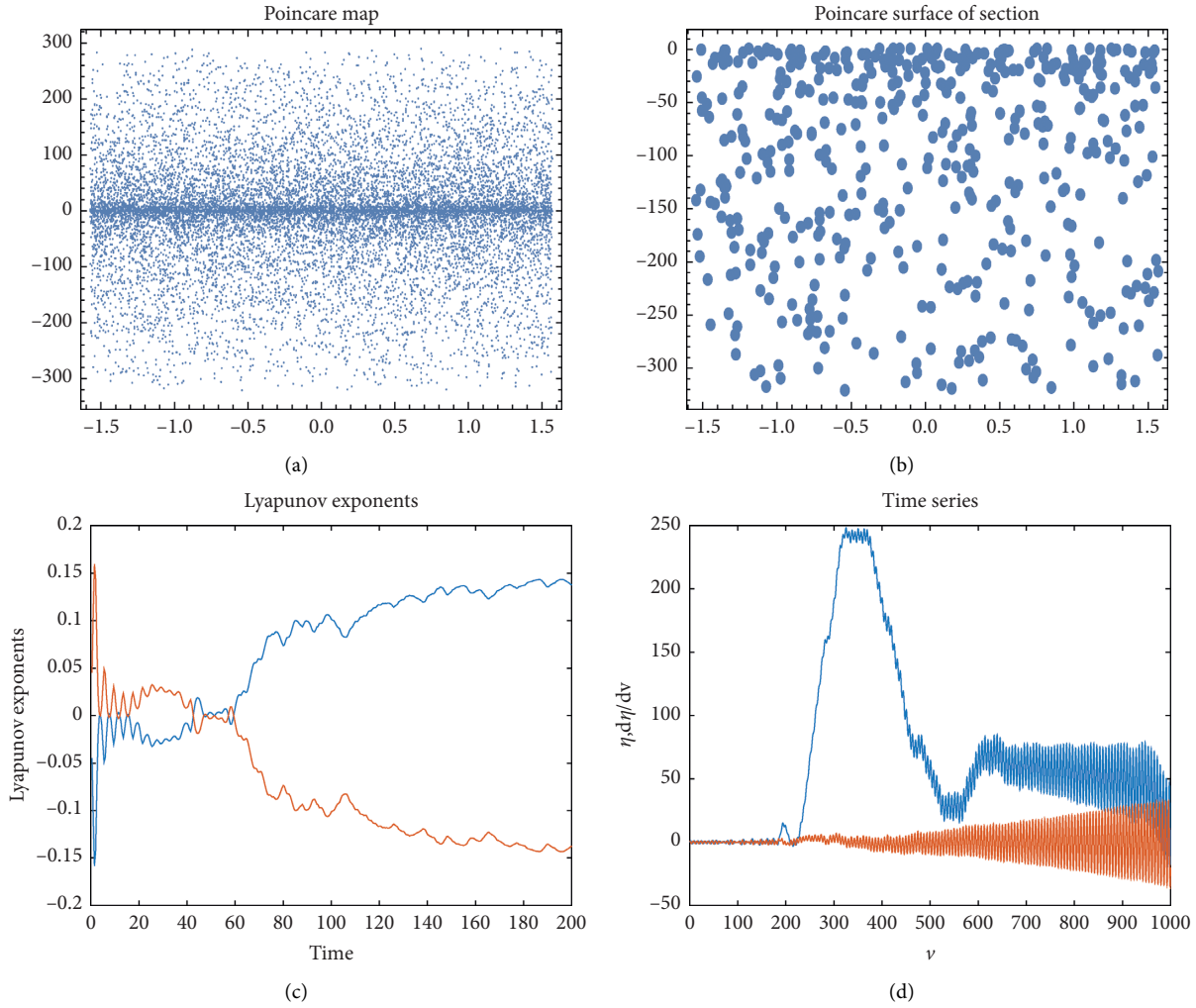

Figure 5: For $n = 0.9, \varepsilon = 0.00000000000001, A_* = 3.36E + 09, D_* = -4E + 08$, $B_* = 1596.387, C_* = -103631, E_* = 200.1022$, and $e = 0.001$. (a) Poincare map, (b) Poincare surface of section, (c) Lyapunov exponent, and (d) time series.

Table 2: Earth-Resourcesat-1 system for fixed values of $A_* = 3.36E + 09, B_* = 1596.387, C_* = -103631, D_* = -4E + 08, E_* = 200.1022, e = 0.001, n$, and variation in ε.

Figure no.	ε	n	Graphical behaviour of Poincare map	Graphical behaviour of Lyapunov exponent
6	0.00000000000000000000000005	0.00001	Curves behave chaotically but remains almost same	Chaotic
7		0.005		Chaotic
8	0.000000000000000000005	0.4		Periodic and chaotic
9		0.8		Periodic

as $t \longrightarrow \pm\infty$, $(dx_p/dt) = 0$ as $x_p \longrightarrow \pm\pi$ are consequently higher subsidiaries of x_p way to deal with zero. As x_p ways to deal with $\pm\pi$, t watches out for uncertain capacity of x_p. This is case of boundless period separatrix.

We presumed that because of the aftereffects of type 1, type 2, and type 3, the streamlined force assumes a huge part in changing the movement of upset to libration or to boundless period separatrix.

2.2. Category-II: $c_{1p} < 2k_{1p}^2$. For this situation, unperturbed arrangement is $x_p = c_{1p} \sin l_p + o(c_{1p}^3)$, $l_p = n_p t + \varepsilon_1$, and $n_p = k_{1p}(1 - (1/16)c_{1p}^2 + \cdots)$, where c_{1p} and ε_1 are the discretionary constants, and l_p is a contention. If there should arise an occurrence of bothered pendulum by utilizing the hypothesis of variety of boundaries, we get $k_p = (\partial/\partial c_{1p})(n_p(\partial x/\partial l))(\partial x/\partial l) - n_p(\partial^2 x/\partial l^2)(\partial x/\partial c_{1p})$, $k_p \cong k_{1p} c_{1p}$,

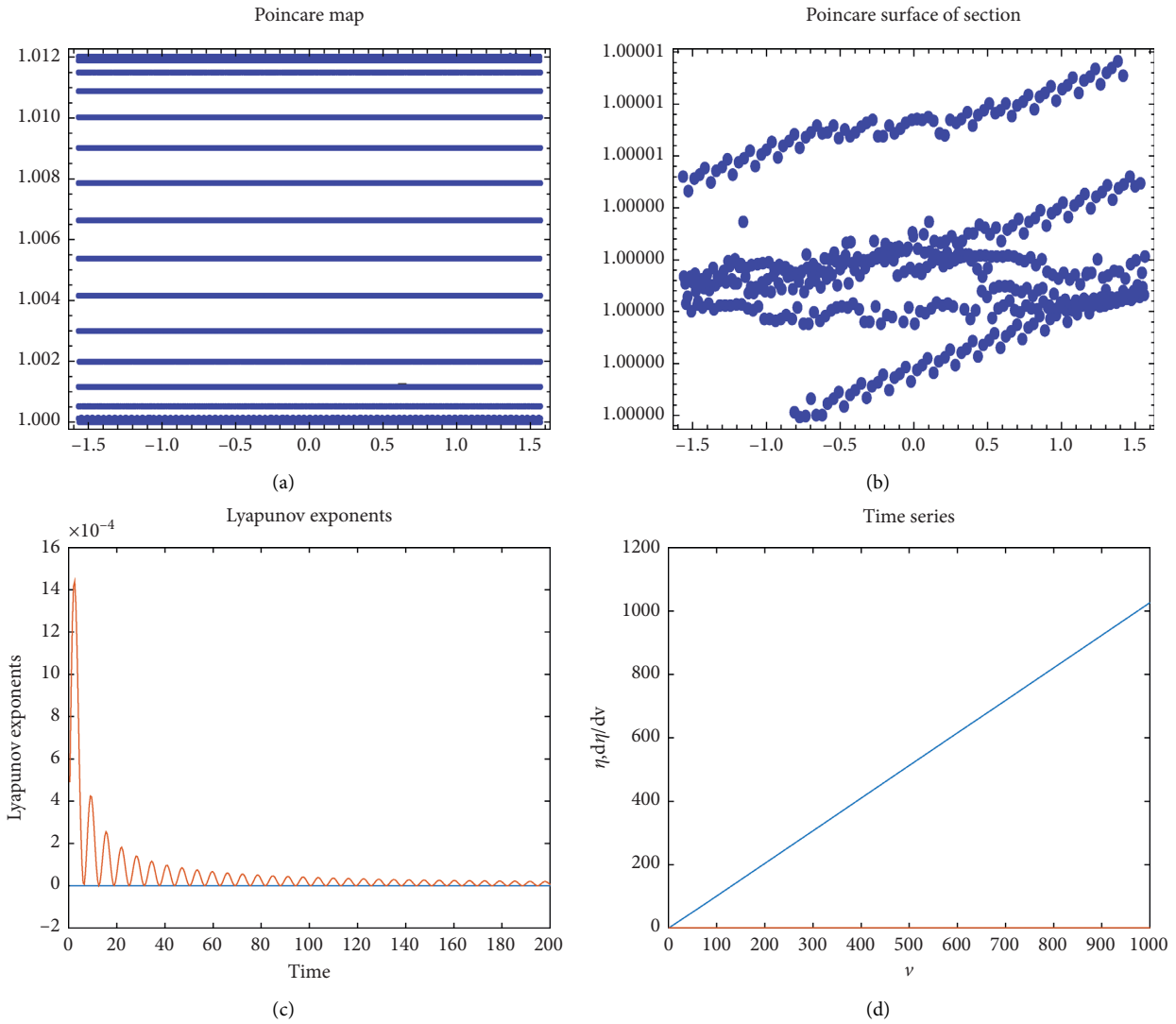

FIGURE 6: For $n = 0.00001, \varepsilon = 0.00000000000000000000000005, A_* = 3.36E + 09, \quad D_* = -4E + 08, B_* = 1596.387, C_* = -103631, E_* = 200.1022$, and $e = 0.001$. (a) Poincare map, (b) Poincare surface of section, (c) Lyapunov exponent, and (d) time series.

$$\begin{aligned}
\frac{d^2 l_p}{dt^2} &= \frac{m_p}{k_{1p}c_{1p}}\left(-C_* - D_* + \frac{m_p E_*^2}{k_{1p}c_{1p}^2}\right)\sin l_p \\
&\quad - \frac{m_p}{c_{1p}}\left(C_* \sin t + D_* t + E_*\right) \\
&\quad + \frac{m_p^2}{k_{1p}^2 c_{1p}^2}\left(C_* E_* \sin t + D_* E_* t + E_*^2\right), \\
\Rightarrow \frac{d^2 l_p}{dt^2} + k_{3p}^2 \sin l_p &= -\frac{m_p}{c_{1p}}\left(C_* \sin t + D_* t + E_*\right) \\
&\quad + \frac{m_p^2}{k_{1p}^2 c_{1p}^2}\left(C_* E_* \sin t + D_* E_* t + E_*^2\right),
\end{aligned} \tag{14}$$

where $k_{3p}^2 = -(m_p/k_{1p}c_{1p})(-C_* - D_* + (m_p E_*^2/k_{1p}c_{1p}^2))$. The unperturbed part of the equation is $((d^2 l_p)/dt^2) + k_{3p}^2 \sin l_p = 0$, where l_p is little, and the arrangement of above condition is $l_p = e^{k_{3p}t} + e^{-k_{3p}t}$. It is again a condition of a pendulum, and as in a prior case, the movement is alluded as upset, libration, and boundless period separatrix.

2.3. Category-III: $c_{1p} = 2k_{1p}^2$. The unperturbed arrangement is

$$x_p + \pi = 4 \tan^{-1} \exp\left(k_{1p}t + \alpha_0\right), \tag{15}$$

where α_0 is a discretionary steady. This is the situation of endless period separatrix as asymptotic forward and in reverse so as to insecure harmony. In this class, the idea of unperturbed arrangement does not change by considering the streamlined force. Close to the endless period, separatrix

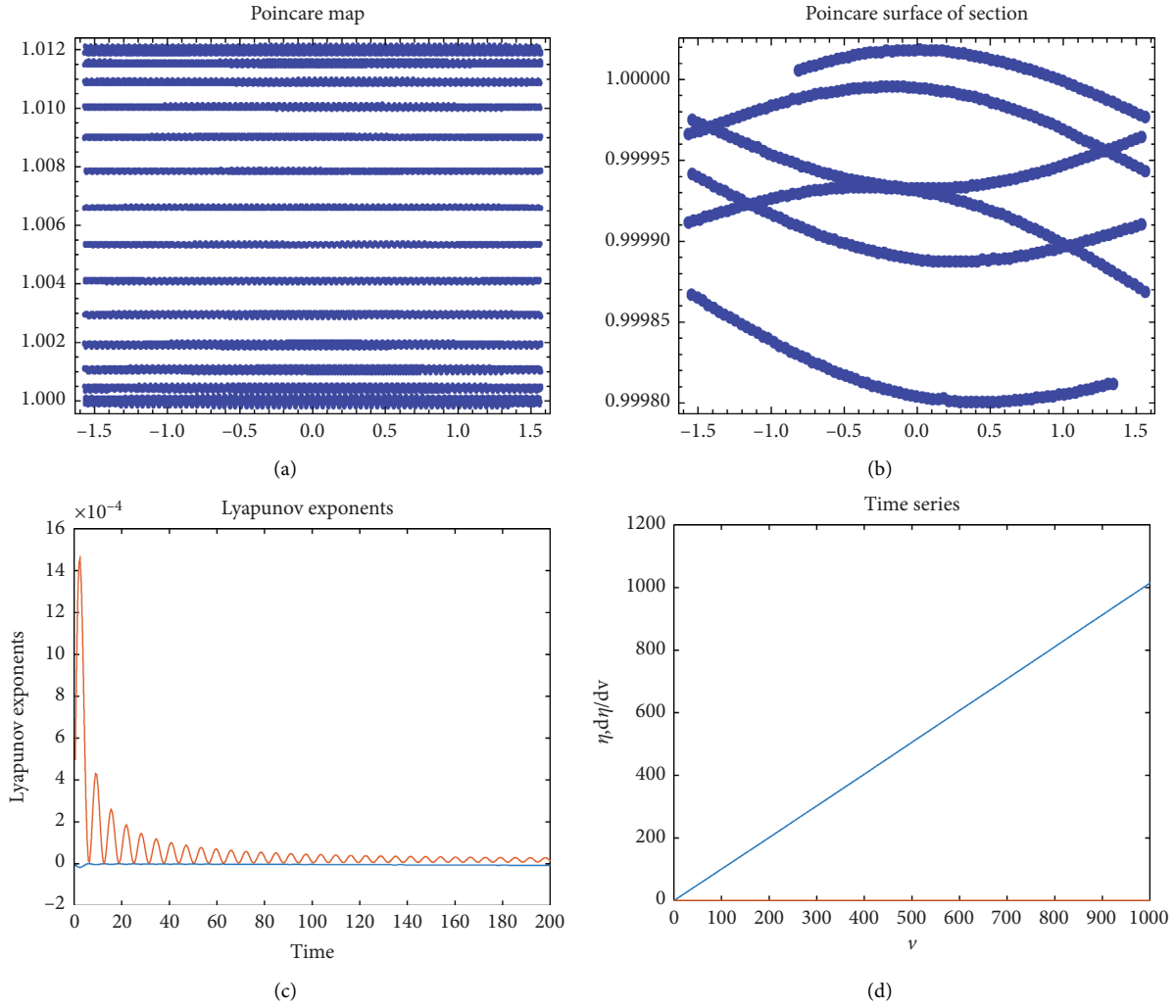

FIGURE 7: For $n = 0.005, \varepsilon = 0.00000000000000000005, A_* = 3.36E + 09, \quad D_* = -4E + 08, B_* = 1596.387, C_* = -103631, E_* = 200.1022$, and $e = 0.001$. (a) Poincare map, (b) Poincare surface of section, (c) Lyapunov exponent, and (d) time series.

widened by high recurrence term into tight clamorous band for little n, and half width of disordered separatrix is given by

$$\omega_p = \frac{I_p - I_p^s}{I_p^s} = 4\pi\varepsilon_1\lambda^3 e^{-(\pi\lambda/2)}, \tag{16}$$

where ε_1 is the proportion of coefficient of closest annoying high-recurrence term to coefficient of perturbed term, and $\lambda = \Omega/\omega$ is the proportion of recurrence distinction between full term and closest nonfull term (Ω) to recurrence of little sufficiency freedoms (ω).

3. Spin-Orbit Phase Space

Utilizing Poincare surface of the segment by taking a gander at directions stroboscopically with period 2π, the segment is drawn with $(d\eta/dv)$ versus v at each periapse section. On account of semi-intermittent direction, focuses are contained in smooth bends, while for clamorous directions, they seem to the top off region in the stage space in an arbitrary way. Since direction indicated by η is identical to the direction signified by $\pi + \eta$, we have, consequently, confined the span from 0 to π.

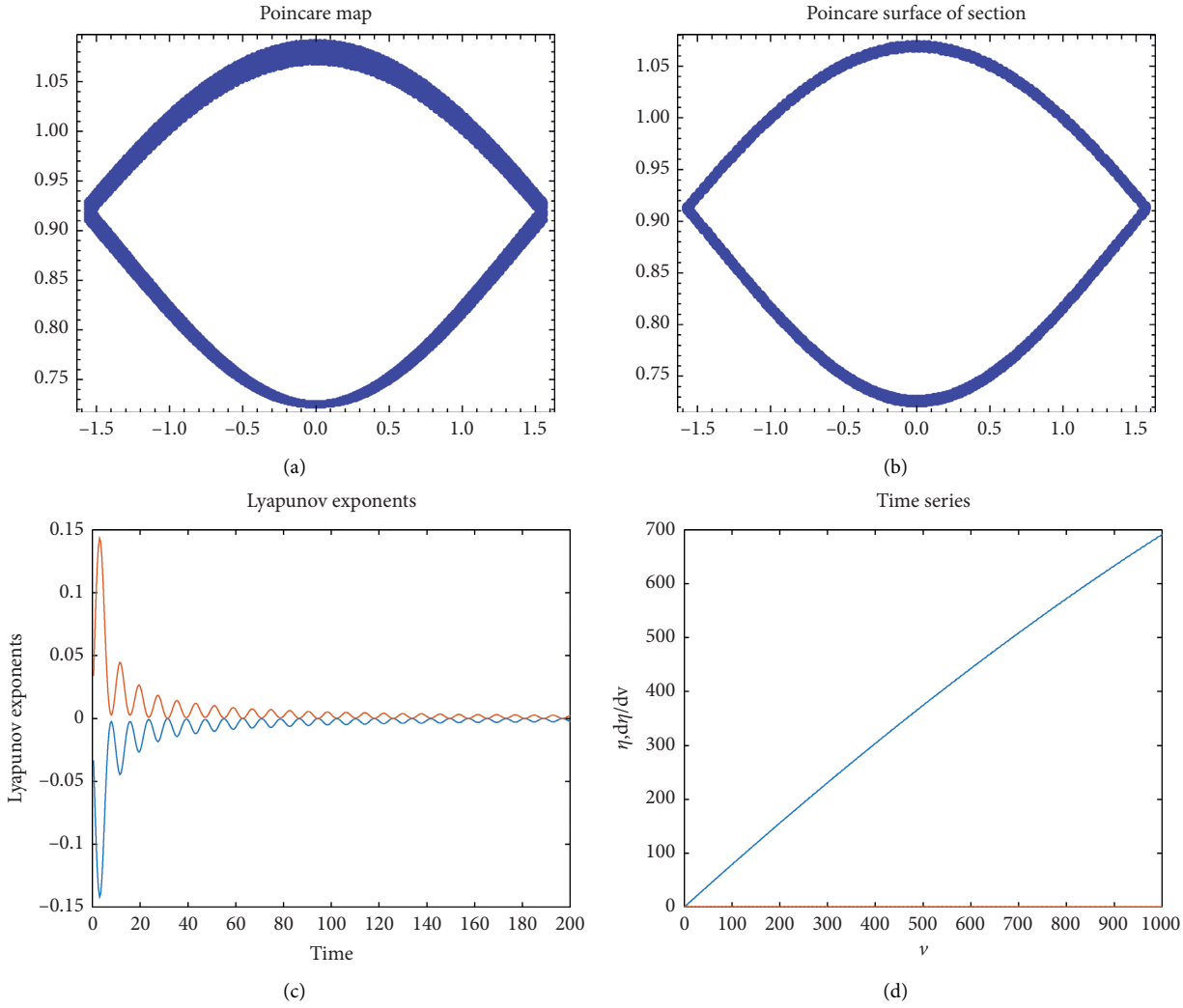

FIGURE 8: For $n = 0.4, \varepsilon = 0.00000000000000000005, A_* = 3.36E + 09, D_* = -4E + 08, B_* = 1596.387, C_* = -103631, E_* = 200.1022$, and $e = 0.001$. (a) Poincare map, (b) Poincare surface of section, (c) Lyapunov exponent, and (d) time series.

4. Results and Discussion

Poincare map, surface of section, and Lyapunov exponents have been plotted for Earth's artificial satellite Resourcesat-1. For the satellite, it is assumed that semimajor axis = $a = 7.195^*10^3$ km, flightiness = $e = 0.001$, tendency = $i = 98.69^\circ$, and angular velocity = $\Omega = 1.034^*10^{-3}$ rad/sec. The effect of mass parameter (n) and aerodynamic torque parameter (ε) is studied on the nonstraight wavering of a satellite in an elliptic circle. Poincare maps, surface of section, Lyapunov exponents, and time series for different values of mass parameter and aerodynamic toque parameter are plotted as described in tables and figures. Table 1 gives the details of figures for Earth − Resourcesat − 1 for fixed values of A_*, $B_*, C_*, D_*, E_*, \varepsilon$, and e, and the variation of values of n from $0 \le n \le 1$ is shown in Figures 2–5. Table 2 gives description of figures for the Earth-Resourcesat-1 system at fixed values of parameters, n, and e, and the variation of values of ε from

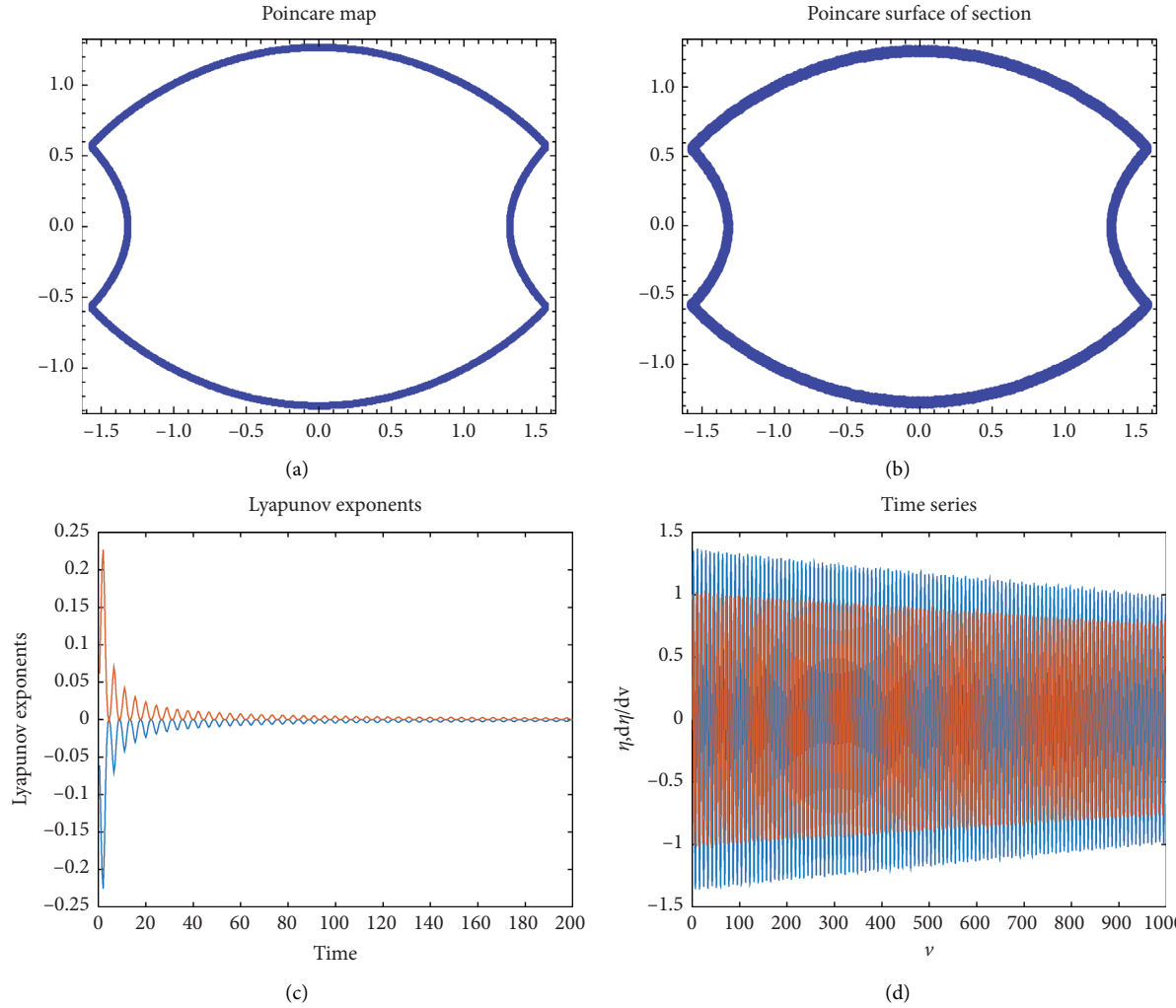

Figure 9: For $n = 0.8, \varepsilon = 0.000000000000000000005, A_* = 3.36E + 09, D_* = -4E + 08, B_* = 1596.387, C_* = -103631, E_* = 200.1022$, and $e = 0.001$. (a) Poincare map, (b) Poincare surface of section, (c) Lyapunov exponent, and (d) time series.

$0 \leq \varepsilon \leq 0.5$ which are plotted is shown in Figures 6–9. From the plots, it is observed that regular curves disintegrate, and this disintegration increases as ε increases and curves behaves chaotically but remains almost same.

5. Conclusion

From these investigations, we conclude that the streamlined force assumes an extremely huge function in changing the movement of insurgency into movement of libration or endless period separatrix. Likewise, we see that standard movement changes into a turbulent one for certain estimations of the streamlined force boundary and mass boundary n. Half width of disordered separatrices assessed by Chirikov's basis is not influenced by the streamlined force. It was seen that counterfeit satellite's turn circle stage space is overwhelmed by a chaotic zone which increments further because of the streamlined force. It is additionally seen that normal bends begin breaking down because of the streamlined force and mass boundary, and this deterioration increments as the streamlined force and mass boundary increments. It is concluded that aerodynamic torque and n change regular movement to the chaotic motion.

Data Availability

No data were used to support this study.

Conflicts of Interest

The authors declare that they have no conflicts of interest.

References

[1] https://www.isro.gov.in/Spacecraft/irs-p6-resourcesat-1 - 14 May 2020.

[2] V. S. Aslanov, A. K. Misra, and V. V. Yudintsev, "Chaotic attitude motion of a low-thrust tug-debris tethered system in a Keplerian orbit," *Acta Astronautica*, vol. 139, pp. 419–427, 2017.

[3] R. Bhardwaj and M. Kaur, "Aerodynamic Torque exhibits non-resonance oscillation in satellite motion," *Mathematica*

Applicanda (Applied Mathematics), vol. 44, no. 2, pp. 247–262, 2016.

[4] R. Bhardwaj and P. Kaur, "Chaotic attitude tumbling of satellite in magnetic field," *American Journal of Applied Sciences*, vol. 3, no. 10, pp. 2037–2041, 2006.

[5] R. Bhardwaj and M. Sethi, "Resonance in satelliteâ€s motion under air drag," *American Journal of Applied Sciences*, vol. 3, no. 12, pp. 2184–2189, 2006.

[6] R. Bhardwaj, M. Sethi, and P. Kaur, "Rotational motion of a satellite under the influence of aerodynamic or magnetic torque," in *Modern Mathematical Methods and Algorithms for Real World Systems*, A. H. Siddiqi, I. S. Duff, and O. Christensen, Eds., pp. 174–184, Anamaya Publishers, Lado Sarai - Mehrauli, Delhi, 2006.

[7] R. Bhardwaj and R. Tuli, "Non-linear planar oscillation of a satellite leading to chaos under the influence of third-body torque," in *Mathematical models and Methods for Real World Systems*, K. M. Furati and A. H. Siddiqi, Eds., Chapman & Hall/ CRC, Boca Raton, Florida, pp. 301–336, 2005.

[8] R. Bhardwaj and P. Kaur, "Chaos in non-linear oscillation of a satellite in elliptic orbit under magnetic torque," in *International Workshop on Applications of Wavelets to Real World Problems*, A. Siddiqui, Ed., pp. 240–258, Istanbul Commerce University Publication, Istanbul, Turkey, 2005.

[9] R. Bhardwaj and K. B. Bhatnagar, "Nonlinear planar oscillation of a satellite in a circular orbit under the influence of magnetic torque (II)," *Indian Journal of Pure & Applied Mathematics*, vol. 29, no. 2, pp. 139–150, 1998.

[10] R. Bhardwaj and K. B. Bhatnagar, "Chaos in nonlinear planar oscillation of a satellite in an elliptical orbit under the influence of third body torque," *Indian Journal of Pure & Applied Mathematics*, vol. 28, no. 3, pp. 391–422, 1997.

[11] R. Bhardwaj and K. B. Bhatnagar, "Nonlinear planar oscillation of a satellite in a circular orbit under the influence of magnetic torque (I)," *Indian Journal of Pure & Applied Mathematics.*vol. 26, no. 12, pp. 1225–1240, 1995.

[12] K. B. Bhatnagar and R. Bhardwaj, "Rotational motion of a satellite on an elliptical orbit under the influence of third body torque (I)," *Bulletin of Astronomical Society of India*, vol. 22, pp. 359–367, 1994.

[13] M. Chegini, H. Sadati, and H. Salarieh, "Chaos analysis in attitude dynamics of a flexible satellite," *Nonlinear Dynamics*, vol. 93, no. 3, pp. 1421–1438, 2018.

[14] M. Chegini, H. Sadati, and H. Salarieh, "Analytical and numerical study of chaos in spatial attitude dynamics of a satellite in an elliptic orbit," in *Proceedings of the Institution of Mechanical Engineers, Part C: Journal of Mechanical Engineering Science*vol. 233, no. 2, pp. 561–577, 2019.

[15] P. T. Clemson and A. Stefanovska, "Discerning non-autonomous dynamics," *Physics Reports*, vol. 542, no. 4, pp. 297–368, 2014.

[16] A. V. Doroshin, "Heteroclinic chaos and its local suppression in attitude dynamics of an asymmetrical dual-spin spacecraft and gyrostat-satellites. The part I-main models and solutions," *Communications in Nonlinear Science and Numerical Simulation*, vol. 31, no. 1-3, pp. 151–170, 2016.

[17] S. A. Gutnik and V. A. Sarychev, "Mathematical simulation of satellite motion with an aerodynamic attitude control system influenced by active damping torques," *Computational Mathematics and Mathematical Physics*, vol. 60, no. 10, pp. 1721–1729, 2020.

[18] M. Iñarrea and V. Lanchares, "Chaotic pitch motion of an asymmetric non-rigid spacecraft with viscous drag in circular orbit," *International Journal of Non-linear Mechanics*, vol. 41, no. 1, pp. 86–100, 2006.

[19] V. Kouprianov and I. Shevchenko, "Rotational dynamics of planetary satellites: a survey of regular and chaotic behavior," *Icarus*, vol. 176, no. 1, pp. 224–234, 2005.

[20] P. V. Kuptsov and S. P. Kuznetsov, "Lyapunov analysis of strange pseudohyperbolic attractors: angles between tangent subspaces, local volume expansion and contraction," *Regular and Chaotic Dynamics*, vol. 23, no. 7-8, pp. 908–932, 2018.

[21] C. Letellier, *Chaos in Nature World Scientific Series on Nonlinear Science Series A*, Vol. 94, World Scientific Publishing, Singapore, 2nd edition, 2019.

[22] J. Liu and N. Cui, "Rigid-flexible coupled dynamics analysis for solar sails," in *Proceedings of the Institution of Mechanical Engineers, Part G: Journal of Aerospace Engineering*vol. 233, no. 1, pp. 324–340, 2019.

[23] A. V. Melnikov and I. I. Shevchenko, "Chaotic dynamics of satellite systems," *Solar System Research*, vol. 39, no. 4, pp. 322–332, 2005.

[24] D. Pritykin, S. Efimov, and V. Sidorenko, "Defunct satellites in nearly polar orbits: long-term evolution of attitude motion," *Open Astronomy*, vol. 27, no. 1, pp. 264–277, 2018.

[25] A. J. Rosengren, E. M. Alessi, A. Rossi, and G. B. Valsecchi, "Chaos in navigation satellite orbits caused by the perturbed motion of the Moon," *Monthly Notices of the Royal Astronomical Society*, vol. 449, no. 4, pp. 3522–3526, 2015.

[26] S. A. Rawashdeh, "Attitude analysis of small satellites using model-based simulation," *International Journal of Aerospace Engineering*, vol. 2019, Article ID 3020581, 2019.

[27] S. Efimov, D. Pritykin, and V. Sidorenko, "Long-term attitude dynamics of space debris in Sun-synchronous orbits: Cassini cycles and chaotic stabilization," *Celestial Mechanics and Dynamical Astronomy*, vol. 130, no. 10, p. 62, 2018.

[28] S.-C. Chang, "Stability, chaos detection, and quenching chaos in the swing equation system," *Mathematical Problems in Engineering*, vol. 2020, Article ID 6677084, 2020.

[29] J. Wang, W. Yu, J. Wang, Y. Zhao, J. Zhang, and D. Jiang, "A new six-dimensional hyperchaotic system and its secure communication circuit implementation," *International Journal of Circuit Theory and Applications*, vol. 47, no. 5, pp. 702–717, 2019.

[30] A. Wolf, J. B. Swift, H. L. Swinney, and J. A. Vastano, "Determining lyapunov exponents from a time series," *Physica D: Nonlinear Phenomena*, vol. 16, no. 3, pp. 285–317, 1985.

[31] J. Wisdom, S. J. Peale, and F. Mignard, "The chaotic rotation of Hyperion," *Icarus*, vol. 58, no. 2, pp. 137–152, 1984.

[32] A. Cayley, "Tables of the developments of functions in the theory of elliptic motion," *Memoirs of the Royal Astronomical Society*, vol. 29, p. 191, 1859.

[33] P. Goldreich and S. Peale, "Spin-orbit coupling in the solar system," *The Astronomical Journal*, vol. 71, p. 425, 1966.

[34] E. W. Brown and C. A. Shook, *Planetary Theory*, Dover Publication. Inc., New York, USA, 1964.